Nucleophilic Addition of Alcohols to $[Fe_2(CO)_6(\mu\text{-}PPh_2)\{\mu\text{-}\eta^1\text{:}\eta^2{}_{\alpha\beta}\text{-}(R)C_\alpha{=}C_\beta{=}C_\gamma H_2\}]$ (R = H, Ph): Generation of the Binuclear β,γ-Unsaturated Esters $[Fe_2(CO)_5(\mu\text{-}PPh_2)(\mu\text{-}\eta^1(O)\text{:}\eta^1(C)\text{:}\eta^2(C)\text{-}\{R^1O(O)CCH_2\}C{=}CH_2)]$ (R^1 = Me, Et, ^{i}Pr)

Simon Doherty,*,† Mark R. J. Elsegood, William Clegg, and Dirk Mampe

Department of Chemistry, Bedson Building, The University of Newcastle upon Tyne, Newcastle upon Tyne, NE1 7RU, United Kingdom

Received September 30, 1996⊗

Nucleophilic addition of alcohols to the μ-η^1:η^2-allenyl complexes $[Fe_2(CO)_6(\mu\text{-}PPh_2)\{\mu\text{-}\eta^1\text{:}\eta^2{}_{\alpha\beta}\text{-}(R)C_\alpha{=}C_\beta{=}C_\gamma H_2\}]$ (R = H, **1a**; R = Ph, **1b**) occurs exclusively *via* a carbonyl−alcohol−allenyl coupling sequence to afford the binuclear β,γ-unsaturated esters $[Fe_2(CO)_5(\mu\text{-}PPh_2)(\mu\text{-}\eta^1(O)\text{:}\eta^1(C)\text{:}\eta^2(C)\text{-}\{R^1O(O)CCHR\}C{=}CH_2)]$ (**2a**, R = H, R^1 = Me; **2b**, R = H, R^1 = Et; **2c**, R = H, R^1 = ^{i}Pr; **2d**, R = Ph, R^1 = Me) which contain a five-membered metallacycle by virtue of coordination of the ester carbonyl. Trimethyl phosphite readily substitutes the metal-coordinated ester carbonyl of **2a**−**c** to afford the ester-functionalized μ-η^1:η^2-alkenyl complexes $[Fe_2(CO)_5\{P(OMe)_3\}(\mu\text{-}PPh_2)(\mu\text{-}\eta^1\text{:}\eta^2\text{-}\{R^1O(O)CCH_2\}C{=}CH_2)]$ (**3a**, R^1 = Me; **3b**, R^1 = Et; **3c**, R^1 = ^{i}Pr). The X-ray structures for **2c**, **2d**, and **3c** are reported.

Introduction

Mononuclear iron complexes of unsaturated carbonyl compounds have demonstrated an impressive versatility in the synthesis of several important classes of organic product.[1] In particular the early studies of Thomas and co-workers rapidly established strategies for the preparation of practical organometallic reagents such as vinyl ketone[2] and (vinylketene)tricarbonyliron(0)[3] complexes, and since their discovery such complexes have been applied to the synthesis of numerous organic products. In many cases these reactions involve the addition of nucleophiles either at a carbonyl to afford, after subsequent coupling, acylated products[4] or directly at the coordinated hydrocarbon to afford a functionalized organic product.[5] In particular, the reactivity of (vinylketene)tricarbonyliron(0) complexes toward nucleophilic substrates was shown to closely parallel that of free vinylketene, namely nucleophilic addition to C1, to afford novel α-substituted-β,γ-unsaturated carbonyl derivatives while their (vinylketenimine)tricarbonyliron(0)[5a] counterparts underwent addition to C2 to afford, after oxidative workup, α,α-dialkyl-β,γ-unsaturated amides.[5b] While these and other mononuclear iron complexes have found widespread use in organic synthesis, there are surprisingly few reports of the successful application of diiron complexes in metal-mediated synthesis although one recent noteworthy example from Gilbertson's laboratory involves the stereo- and regioselective [3+2] cycloaddition of nitrones with diiron α,β-unsaturated acyl complexes to afford isoxazilidines.[6]

Diiron allenyl complexes are particularly attractive candidates for use in synthesis because they contain the cumulated fragment $C(H){=}C{=}CH_2$, a potentially versatile building block for the synthesis of a wide range of organic products.[7] We noted that a recent attempt to prepare the diiron allenyl complex $[Fe_2(CO)_6(\mu\text{-}PPh_2)\{\mu\text{-}\eta^1\text{:}\eta^2\text{-}(^t\text{Bu})C{=}C{=}CH_2\}]$ from the nucleophilic addition of diazomethane to C_α of the acetylide in $[Fe_2(CO)_6(\mu\text{-}PPh_2)(\mu\text{-}\eta^1\text{:}\eta^2\text{-}C{\equiv}C^t\text{Bu})]$ led to the facile addition of 2 equiv of CH_2 to afford the butadienylidene complex $[Fe_2(CO)_5(\mu\text{-}PPh_2)\{\mu\text{-}\eta^1\text{:}\eta^2\text{:}\eta^2\text{-}CH_2C(^t\text{Bu})C{=}CH_2\}]$, presumably *via* the desired but kinetically reactive allenyl complex.[8] This suggested to us that, if accessible, such allenyl complexes would be highly reactive, possibly opening new avenues of reactivity associated with carbon−carbon and carbon−heteroatom coupling reactions.

With this in mind we have recently succeeded in preparing $[Fe_2(CO)_6(\mu\text{-}PPh_2)\{\mu\text{-}\eta^1\text{:}\eta^2{}_{\alpha\beta}\text{-}(H)C_\alpha{=}C_\beta{=}C_\gamma H_2\}]$ (**1a**), and a preliminary evaluation of its reactivity has demonstrated new reaction pathways for μ-η^1:η^2-allenyl ligands including regiospecific attack of phosphorus nucleophiles at C_α to afford, after 1,4-hydrogen migra-

† e-mail: simon.doherty@newcastle.ac.uk.

⊗ Abstract published in *Advance ACS Abstracts,* February 15, 1997.

(1) (a) Davies, S. G. *Organotransition Metal Chemistry: Applications to Organic Synthesis*; Pergamon Press: Oxford, 1982. (b) Pearson, A. J. *Metallo-Organic Chemistry*; Wiley: Chichester, 1985. (c) Brunet, J.-J. *Chem. Rev.* **1990**, *90*, 1041. (d) Khumtaveepron, K.; Alper, H. *Acc. Chem. Res.* **1995**, *28*, 414.

(2) Thomas, S. E. *J. Chem. Soc., Chem. Commun.* **1987**, 226.

(3) (a) Alcock, N. W.; Richards, C. J.; Thomas, S. E. *Organometallics* **1991**, *10*, 231. (b) Alcock, N. W.; Danks, T. N.; Richards, C. J.; Thomas, S. E. *J. Chem. Soc., Chem. Commun.* **1989**, 21.

(4) (a) Danks, T. N.; Rakshit, D.; Thomas, S. E. *J. Chem. Soc., Perkin Trans. 1* **1988**, 2091. (b) Pouilhes, A.; Thomas, S. E. *Tetrahedron Lett.* **1989**, *30*, 2285. (c) Thomas, S. E.; Tustin, G. J.; Ibbotson, A. *Tetrahedron*, **1992**, *48*, 7629. (d) Gibson S. E.; Tustin, G. *J. Chem. Soc., Perkin Trans. I* **1995**, 2427.

(5) (a) Hill, L.; Richards, C. J.; Thomas, S. E. *J. Chem. Soc., Chem. Commun.* **1990**, 1085. (b) Richards, C. J.; Thomas, S. E. *J. Chem. Soc., Chem. Commun.* **1990**, 307.

(6) Gilbertson, S. R.; Dawson, D. P.; Lopez, O. D.; Marshall, K. L. *J. Am. Chem. Soc.* **1995**, *117*, 4431.

(7) For recent comprehensive reviews see: (a) Wojcicki, A. *New. J. Chem.* **1994**, *18*, 61. (b) Doherty, S.; Corrigan, J. F.; Carty, A. J.; Sappa, E. *Adv. Organomet. Chem.* **1995**, *37*, 39.

(8) Breckenridge, S. M.; MacLaughlin, S. A.; Taylor, N. J.; Carty, A. J. *J. Chem. Soc., Chem. Commun.* **1991**, 1718.

(9) (a) Doherty, S.; Elsegood, M. R. J.; Clegg, W.; Scanlan, T. H.; Rees, N. H. *J. Chem. Soc., Chem. Commun.* **1996**, 1545. (b) Doherty, S.; Elsegood, M. R. J.; Clegg, W.; Mampe, D.; Rees, N. H. *Organometallics* **1996**, *15*, 5302.

S0276-7333(96)00832-1 CCC: $14.00

Scheme 1

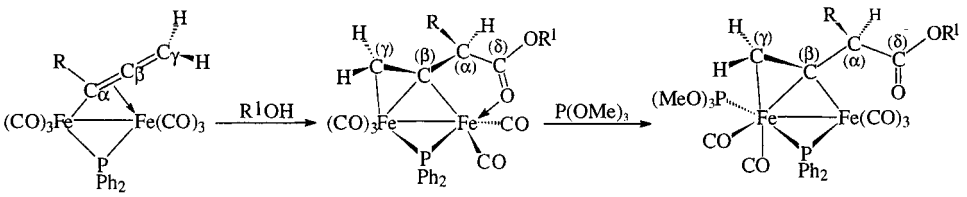

R = H, R¹ = Me, **2a**; R = H, R¹ = Et, **2b**
R = H, R¹ = ⁱPr; **2d**; R = Ph, R¹ = Me; **2d**

R = H, R¹ = Me, **3a**
R = H, R¹ = Et, **3b**
R = H, R¹ = ⁱPr; **3c**

tion, phosphino-substituted μ-η^1:η^2-alkenyl complexes[9] and competitive nucleophilic attack of primary amines at CO and C_β of the allenyl ligand to afford amido-functionalized alkenyl complexes and dimetallacyclopentanes, respectively.[10] As part of our ongoing investigation into the general reactivity of **1** with nucleophiles we have examined the reactivity of diiron allenyl complexes toward alcohols. Herein we report that alcohols react with diiron μ-η^1:η^2-allenyl complexes with impressive selectivity *via* nucleophilic attack at a carbonyl followed by allenyl carbonyl coupling to afford the β,γ-unsaturated carbonyl derivatives $[Fe_2(CO)_5(\mu\text{-}PPh_2)(\mu\text{-}\eta^1(O):\eta^1(C):\eta^2(C)\text{-}\{R^1O(O)CCRH\}C{=}CH_2)]$. The successful transformation of a μ-η^1:η^2-allenyl ligand into an β,γ-unsaturated ester represents an attractive alternative to their synthesis from vinylketenetricarbonyliron(0) complexes described by Thomas.[5]

Results and Discussion

Synthesis. The binuclear allenyl complexes $[Fe_2(CO)_6(\mu\text{-}PPh_2)\{\mu\text{-}\eta^1:\eta^2{}_{\alpha\beta}\text{-}(R^1)C_\alpha{=}C_\beta{=}C_\gamma H_2\}]$ (R^1 = H, **1a**; R^1 = Ph, **1b**) were synthesized from $Na[Fe_2(CO)_7(\mu\text{-}PPh_2)]$[11] and the corresponding alkynyl bromide as previously described.[9] Unfortunately, we have been unable to isolate and fully characterize $[Fe_2(CO)_6(\mu\text{-}PPh_2)\{\mu\text{-}\eta^1:\eta^2{}_{\alpha\beta}\text{-}(Ph)C_\alpha{=}C_\beta{=}C_\gamma H_2\}]$ (**1b**) because of its rapid decomposition during column chromatography. Thus **1b** was typically generated *in situ* prior to the addition of alcohol.

Complex **1a** reacts with methanol, ethanol, and propan-2-ol regiospecifically to afford in each case, and as the sole product of reaction, the β,γ-unsaturated carbonyl compounds $[Fe_2(CO)_5(\mu\text{-}PPh_2)(\mu\text{-}\eta^1(O):\eta^1(C):\eta^2(C)\text{-}\{R^1O(O)CCH_2\}C{=}CH_2)]$ (**2a**, R^1 = Me; **2b**, R^1 = Et; **2c**, R^1 = ⁱPr) in yields of up to 75% (Scheme 1). The ^{1}H NMR spectra of **2a**−**c** each contain four distinctive sets of resonances corresponding to the diastereotopic methylene protons associated with the μ-η^1:η^2-alkenyl ligand (Table 1). The alkenyl protons ($C_\gamma H_a H_b$) appear as doublets of doublets with large $^2J_{PH}$ (**2a**, 11.5; **2b**, 11.7; **2c**, 11.7 Hz) and small geminal $^2J_{HH}$ (**2a**−**c**, 2.9 Hz) coupling constants while the remaining diastereotopic methylene protons ($C_\alpha H_c H_d$) exhibit much larger geminal couplings (**2a**, 21.6; **2b**, 21.2; **2c**, 21.3 Hz) (Table 1). The $^{13}C\{^1H\}$ NMR spectra of **2a**−**c** contain resonances for C_β and C_γ with chemical shifts that compare favorably with previously reported values for related μ-η^1:η^2-alkenyl ligands.[12] A low-field signal (δ 166.8) for C_β in **2a**−**c** suggests a significant contribution from its carbene resonance structure (**b**), while the high-field signal (δ 63.1, **2a**; 63.1, **2b**; 63.3, **2c**) associated with C_γ is consistent with metallocyclopropane sp^3 character (Table 2). Complexes **2a**−**c** can most aptly be considered as "carbonyl tethered" σ-π-alkenyl complexes and as such cannot undergo site exchange *via* the "windshield-wiper" mechanism.[13] In fact, in addition to cleavage of the "anchoring" metal−carbonyl interaction, such an exchange mechanism would also require internuclear migration of CO.

Table 1. ^{1}H NMR Data for Diiron Alkenyl Complexes 2a−d and 3a−c

compound	R	R¹	δ(H$_a$)	δ(H$_b$)	δ(H$_c$)	δ(H$_d$)	J_{HaHb}/Hz	J_{HcHd}/Hz
2a	H_d	Me	3.21	2.20	4.12	3.06	2.9	21.6
2b	H_d	Et	3.21	2.21	4.11	3.03	2.9	21.2
2c	H_d	ⁱPr	3.31	2.21	4.12	2.97	2.9	21.3
2d	Ph	Me	2.60	2.23	5.12	−	3.7	−
3a	H_d	Me	2.72	2.17	4.22	3.05	4.0	12.2
3b	H_d	Et	2.71	2.15	4.22	3.04	3.1	12.3
3c	H_d	ⁱPr	2.72	2.18	4.18	3.02	3.1	12.4

Table 2. $^{13}C\{^1H\}$ NMR Data for Diiron Alkenyl Complexes 2a−d and 3a−c

compound	R	R¹	δ(C$_\beta$)	δ(C$_\gamma$)	δ(C$_\alpha$)	δ(C$_\delta$)	J_{PC_β}	J_{PC_γ}	J_{PC_α}
2a	H_d	Me	166.8	63.1	53.4	186.6	27.6	8.8	3.7
2b	H_d	Et	166.8	63.1	53.8	186.3	28.9	8.8	3.8
2c	H_d	ⁱPr	166.8	63.3	54.2	186.0	27.7	8.8	3.5
2d	Ph	Me	171.0	68.9	52.3	185.2	21.3	7.6	3.8
3a	H_d	Me	178.5	71.2	61.6	172.8	21.9	14.9, 5.6	6.6
3b	H_d	Et	178.9	71.3	53.3	172.4	22.0	14.3, 5.6	−
3c	H_d	ⁱPr	179.1	71.2	68.1	171.9	21.4	14.2, 5.4	−

X-ray Structure of 2c. Full structural details of **2c** were provided by a single-crystal X-ray analysis, and a perspective view of the molecular structure together with the atomic numbering scheme is illustrated in Figure 1. A selection of bond distances and angles are given in Table 3. The molecular structure confirms that the bridging β,γ-unsaturated ester results from 2-propanol−carbonyl−allenyl coupling together with hydrogen migration to C_α of the allenyl ligand. Interestingly the ester carbonyl oxygen coordinates to Fe(2) forming a five-membered metallacycle with Fe−O (Fe(2)−O(1) = 2.074(2) Å) and C−O (C(4)−O(1) = 1.229(3) Å) bond lengths similar to those recently reported for $[Fe_2(CO)_4\{C(CO_2Me){=}CHC(OMe){=}O\}(\mu\text{-}PPh_2)(\mu\text{-dppm})]$.[14] The remainder of the coordination sphere comprises two

(10) Doherty, S.; Elsegood, M. R. J.; Clegg, W.; Waugh, M. *Organometallics* **1996**, *15*, 2688.
(11) Osterloh, W. T. Ph.D. Thesis, University of Texas, Austin, TX, 1982.
(12) (a) Seyferth, D.; Archer, C. M.; Ruschke, D. P.; Cowie, M.; Hilts, R. W. *Organometallics* **1991**, *10*, 3363. (b) MacLaughlin, S. A.; Doherty, S.; Taylor, N. J.; Carty, A. J. *Organometallics* **1992**, *11*, 4315.
(13) (a) Shapley, J. R.; Richter, S. I.; Tachikawa, M.; Keister, J. B. *J. Organomet. Chem.* **1975**, *94*, C43. (b) Xue, Z.; Sieber, W. J.; Knobler, C. B.; Kaesz, H. B. *J. Am. Chem. Soc.* **1990**, *112*, 1825. (c) Farrugia, L.; Chi, Y.; Tu, W.-C. *Organometallics* **1993**, *12*, 1616.
(14) Hogarth, G.; Lavender, M. H. *J. Chem. Soc., Dalton Trans.* **1994**, 3389.

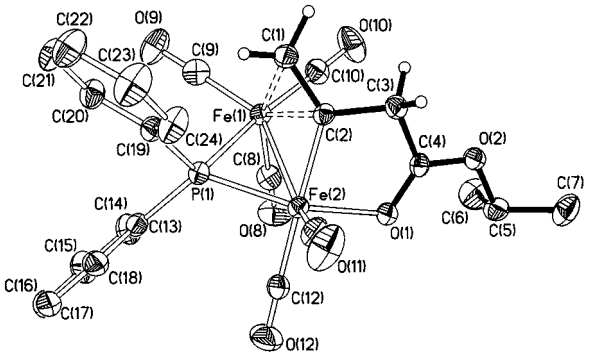

Figure 1. Molecular structure of $[Fe_2(CO)_5(\mu\text{-}PPh_2)(\mu\text{-}\eta^1(O):\eta^1(C):\eta^2(C)\text{-}\{^iPrO(O)CCH_2\}C{=}CH_2)]$ (**2c**) with atom labels and 50% probability ellipsoids. Phenyl and isopropyl H atoms are omitted for clarity.

Table 3. Selected Bond Distances (Å) and Angles (deg) for Compound 2c

Fe(1)−Fe(2)	2.5791(6)	Fe(1)−C(1)	2.179(3)
Fe(1)−C(2)	2.135(3)	Fe(1)−P(1)	2.2590(9)
Fe(1)−C(8)	1.775(3)	Fe(1)−C(9)	1.774(3)
Fe(1)−C(10)	1.795(3)	Fe(2)−C(2)	1.956(3)
Fe(2)−O(1)	2.074(2)	Fe(2)−P(1)	2.1542(9)
Fe(2)−C(11)	1.746(3)	Fe(2)−C(12)	1.798(3)
C(1)−C(2)	1.398(4)	C(2)−C(3)	1.505(4)
C(3)−C(4)	1.482(4)	C(4)−O(1)	1.229(3)
C(4)−O(2)	1.314(3)		
C(2)−Fe(2)−O(1)	82.58(10)	C(1)−C(2)−C(3)	118.7(3)
C(3)−C(2)−Fe(2)	110.6(2)	C(2)−C(3)−C(4)	109.3(2)
O(1)−C(4)−C(3)	121.2(3)	C(4)−O(1)−Fe(2)	112.2(2)
Fe(1)−P(1)−Fe(2)	71.48(3)		

carbonyl ligands, the phosphido bridge and the σ-bonded alkenyl group (Fe(2)−C(2) = 1.956(3) Å). The coordination geometry at Fe(1) is trigonal bipyramidal and consists of three carbonyl ligands, the phosphido bridge and the π-bonded alkenyl group (Fe(1)−C(1) = 2.179(3) Å, Fe(1)−C(2) = 2.135(3) Å). The C(1)−C(2) bond length (1.398(4) Å) is comparable to values in other diiron alkenyl complexes[12] and shows the expected increase upon coordination to a metal center. The σ-η^1-alkenyl group in **2c** adopts an *endo* orientation with respect to the phosphido bridge, presumably to avoid unfavorable steric interactions between the ester functionality of C_β and the phenyl group of the phosphido bridging ligand. The structure of **2c** supports our description of the bridging hydrocarbyl fragment as a μ-η^1:η^2-alkenyl ligand, anchored to iron *via* intramolecular coordination of the ester carbonyl. We note that irradiation of allenic ketones and amides in the presence of $Fe(CO)_5$ has been reported to give the closely related complexes $[Fe_2(CO)_6\{\mu\text{-}\eta^1\text{:}\eta^3\text{-}CR_2CCR^1C(O)X\}]$ (X = OR, NR_2) with a similar interaction of the carbonyl oxygen to a single iron atom, although, in contrast to **2a**−**d** the unsaturated hydrocarbyl ligands are μ-η^1:η^3-coordinated.[15,16]

Isotopic Labeling Studies and X-ray Structure of 2d. The reaction of **1a** with CD_3OD was monitored by ^1H NMR spectroscopy and after several hours three distinct resonances appeared (δ 2.20, 3.05, 3.21 ppm)

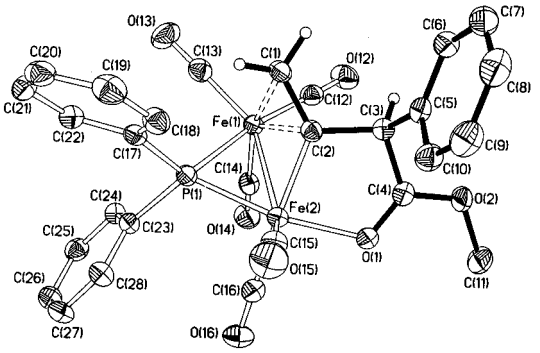

Figure 2. Molecular structure of $[Fe_2(CO)_5(\mu\text{-}PPh_2)(\mu\text{-}\eta^1(O):\eta^1(C):\eta^2(C)\text{-}\{MeO(O)CCHPh\}C{=}CH_2)]$ (**2d**) with atom labels and 50% probability ellipsoids. Phenyl and methyl H atoms are omitted for clarity.

which correspond to the formation of $[Fe_2(CO)_5(\mu\text{-}PPh_2)(\mu\text{-}\eta^1(O):\eta^1(C):\eta^2(C)\text{-}\{MeO(O)CCHD\}C{=}CH_2)]$, $[^2H_1]$-**2a**. Two of these, which appear as well resolved doublets of doublets at δ 3.21 and 2.20, belong to the diastereotopic protons of $C_\gamma H_a H_b$ while the remaining resonance, a single broad ill-defined signal at δ 3.06, corresponds to $C_\alpha D H_d$. These spectroscopic characteriztics are consistent with the formation of a single isotopomer with the deuterium located solely on C_α of the original allenyl fragment. The absence of a resonance at δ 4.12, previously assigned to $C_\alpha H_c H_d$ in d_0-**2a**, together with loss of the characteristically large geminal $^2J_{HH}$ coupling constant supports our formulation for this isotopomer. Additionally, the ^2H NMR spectrum of $[^2H_1]$-**2a** contained a single broad resonance at δ 4.18, confirming our spectroscopic assignment. This labeling experiment supports a reaction sequence involving nucleophilic attack of ROH at CO, carbon−carbon bond formation with C_α of the allenyl ligand, and stereoselective hydrogen transfer to the same carbon, provided that hydrogen scrambling between C_α and C_γ does not occur. The conclusions from this deuterium labeling experiment were further reinforced by the reactivity of $[Fe_2(CO)_6(\mu\text{-}PPh_2)\{\mu\text{-}\eta^1\text{:}\eta^2{}_{\alpha\beta}\text{-}(Ph)C_\alpha{=}C_\beta{=}C_\gamma H_2\}]$ (**1b**) with methanol, details of which are described below.

We have successfully prepared, isolated, and structurally characterized the α-phenyl-β,γ-unsaturated carbonyl complex $[Fe_2(CO)_5(\mu\text{-}PPh_2)(\mu\text{-}\eta^1(O):\eta^1(C):\eta^2(C)\text{-}\{MeO(O)CCHPh\}C{=}CH_2)]$ (**2d**) from the reaction between $[Fe_2(CO)_6(\mu\text{-}PPh_2)\{\mu\text{-}\eta^1\text{:}\eta^2{}_{\alpha\beta}\text{-}(Ph)C_\alpha{=}C_\beta{=}C_\gamma H_2\}]$ (**1b**) and methanol. The ^1H and $^{13}C\{^1H\}$ spectroscopic characteriztics of **2d** are consistent with our formulation as a α-substituted β,γ-unsaturated carbonyl derivative (Tables 1 and 2). Crystals of **2d** suitable for X-ray analysis were grown from CH_2Cl_2/*n*-hexane, and a perspective view of the molecular structure is shown in Figure 2 with a selection of bond lengths and angles listed in Table 4. The molecular structure clearly identifies **2d** as $[Fe_2(CO)_5(\mu\text{-}PPh_2)(\mu\text{-}\eta^1(O):\eta^1(C):\eta^2(C)\text{-}\{MeO(O)CCHPh\}C{=}CH_2)]$ containing a bridging α-substituted β,γ-unsaturated ester σ-bonded to Fe(2) [Fe(2)−C(2) = 1.946(2) Å], π-bonded to Fe(1) [Fe(1)−C(1) = 2.154(2) Å, Fe(1)−C(2) = 2.133(2) Å], and coordinated through the ester carbonyl oxygen to Fe(1) [Fe(2)−O(1) = 2.0486(17) Å], forming an oxametallacycle similar to that in **2c**. The remaining structural characteristics associated with the bridging hydrocarbyl fragment, metal atom framework, and the supporting ligands are similar to those in **2c**. Crystals of **2d** contain a single

(15) (a) Trifonov, L. S.; Orahovats, A. S.; Heimgartner, H. *Helv. Chim. Acta*. **1990**, *73*, 1734. (b) Trifonov, L. S.; Orahovats, A. S.; Prewo, R.; Heimgartner, H. *Helv. Chim. Acta* **1988**, *71*, 551. (c) Trifonov, L. S.; Orahovats, A. S.; Linden, A.; Heimgartner, H. *Helv. Chim. Acta* **1992**, *75*, 1872.

(16) (a) Martina, D.; Brion, F.; De Cian, A. *Tetrahedron Lett*. **1982**, *23*, 857. (b) Brion, F.; Martina, D. *Tetrahedron Lett*. **1982**, *23*, 861.

Table 4. Selected Bond Distances (Å) and Angles (deg) for Compound 2d

Fe(1)−Fe(2)	2.6319(6)	Fe(1)−C(1)	2.154(2)
Fe(1)−C(2)	2.133(2)	Fe(1)−C(12)	1.802(3)
Fe(1)−C(13)	1.786(3)	Fe(1)−C(14)	1.777(3)
Fe(1)−P(1)	2.2501(7)	Fe(2)−C(2)	1.946(2)
Fe(2)−O(1)	2.0486(17)	Fe(2)−P(1)	2.1523(7)
Fe(2)−C(15)	1.755(3)	Fe(2)−C(16)	1.810(3)
C(1)−C(2)	1.400(3)	C(2)−C(3)	1.534(3)
C(3)−C(4)	1.503(3)	C(4)−O(1)	1.226(3)
C(4)−O(2)	1.325(3)		
C(2)−Fe(2)−O(1)	83.04(8)	C(1)−C(2)−C(3)	116.9(2)
C(3)−C(2)−Fe(2)	112.45(16)	C(2)−C(3)−C(4)	107.85(19)
O(1)−C(4)−C(3)	121.1(2)	C(4)−O(1)−Fe(2)	114.15(15)
Fe(1)−P(1)−Fe(2)	73.39(2)		

diastereoisomer with the phenyl substituent located *exo* with respect to the closest carbonyl ligand, C(12)O(12). However, close examination of the proton NMR spectrum of **2c** suggests that a second isomer is present in small amounts (<5%), in solution, as evidenced by three additional sets of methylene resonances with chemical shifts and coupling constants similar to those of **2d**. We tentatively suggest this additional set of resonances to be associated with a minor diastereoisomer of **2d** in which the phenyl substituent on C(3) is *exo* to the phosphido bridge. This isomer would encounter significant steric interactions with the carbonyl ligands on Fe(1).

Phosphine Substitution Reactions and X-ray Structure of 3c. Deep red diethyl ether solutions of **2a**−**c** react with trimethyl phosphite to afford golden yellow/orange solutions of the phosphite substituted μ-η^1:η^2-alkenyl complexes $[Fe_2(CO)_5\{P(OMe)_3\}(\mu\text{-}PPh_2)(\mu\text{-}\eta^1\text{:}\eta^2\text{-}\{R^1O(O)CCH_2\}C{=}CH_2)]$ (**3a**, R^1 = Me; **3b**, R^1 = Et; **3c**, R^1 = ^{i}Pr); isolated in near quantitative yield after chromatographic separation and crystallization from dichloromethane/*n*-hexane. For each compound the $^{31}P\{^1H\}$ NMR spectrum contains a well resolved doublet of doublets with a large $^2J_{PP}$ coupling constant (J = 90.9, **3a**; 88.0, **3b**; 87.1 Hz, **3c**); strongly suggesting that the phosphite and phosphido bridge adopt a *trans* disposition and fully consistent with substitution of the metal coordinated ester oxygen. For **3c**, a minor (<5%) set of ^{31}P resonances (δ 185.2 and 163.2; $^2J_{PP}$ = 84.0 Hz) is likely to correspond to an isomer, possibly that in which the alkenyl ligand is σ-bonded to Fe(1) and π-bonded to Fe(2) (*vide infra*). These two isomers reflect the rigid nature of the σ-π-bound hydrocarbyl bridging ligand which has an unusually high barrier to exchange *via* the windshield wiper mechanism. Such observations are now becoming commonplace with independent reports by Carty,[12b] Hogarth,[17] and Seyferth.[12a,18] The ^1H NMR spectra of **3a**−**c** each contain four diastereotopic methylene signals with distinctly different coupling patterns to those of **2a**−**c** (Table 1). The ^{13}C signals associated with the μ-η^1:η^2-alkenyl ligand in **3a**−**c** are similar to those of **2a**−**c** (Table 2) with one notable difference, an additional phosphorus−carbon coupling which suggests that the trimethyl phosphite coordinates to the η^2-bound iron.

Although the spectroscopic characteristics of **3a**−**c** are consistent with an ester-functionalized μ-η^1:η^2-alkenyl ligand, a single-crystal X-ray analysis of **3c** was carried out to provide precise structural details. We noted that upon standing solutions of **3c** readily lose trimethyl phosphite to regenerate **2d**, and crystals suitable for X-ray analysis could only be grown from dichloromethane/*n*-hexane in the presence of excess trimethyl phosphite. Crystals of **3c** are rhombohedral in the space group R$\bar{3}$. Interestingly six molecules of the diiron complex pack around each $\bar{3}$ (S_6) site to form a channel which contains seven molecules of hexane of crystallization, six of which are symmetry related while the remaining one is disordered about the three-fold axis. A diagram highlighting this packing effect is shown in Figure 3, and a perspective view of the molecular structure together with the atomic numbering scheme is illustrated in Figure 4. A selection of bond distances and angles are listed in Table 5. The most notable feature of **3c** is the μ-η^1:η^2-alkenyl ligand with a pendent ester functionality attached to C_β, which in **2b** was coordinated *via* its carbonyl oxygen to Fe(2). The alkenyl ligand is σ-bonded to Fe(2) (Fe(2)−C(2) = 1.987(3) Å) and π-bonded to Fe(1) (Fe(1)−C(1) = 2.152(3) Å, Fe(1)−C(2) = 2.122(3) Å) with a C−C bond length similar to that in **2c**. As expected, from $^{31}P\{^1H\}$ studies,

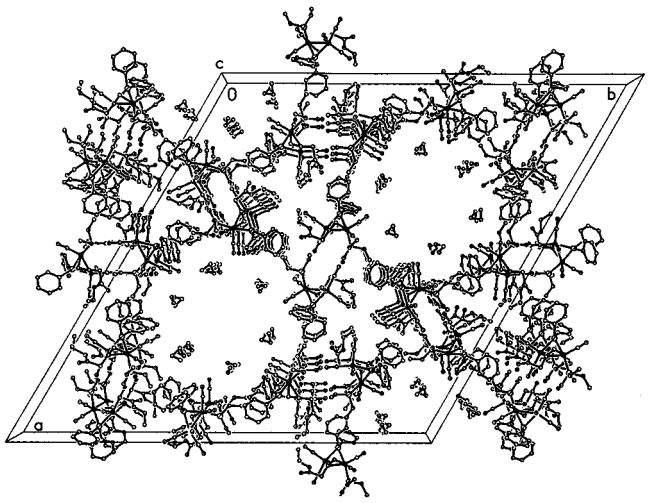

Figure 3. Crystal packing of compound **3c**·$^7/_6$hexane viewed in perspective along the *c* axis, showing the channel occupied by hexane molecules. H atoms are omitted; the disordered hexane on the C_3 axes has not been located.

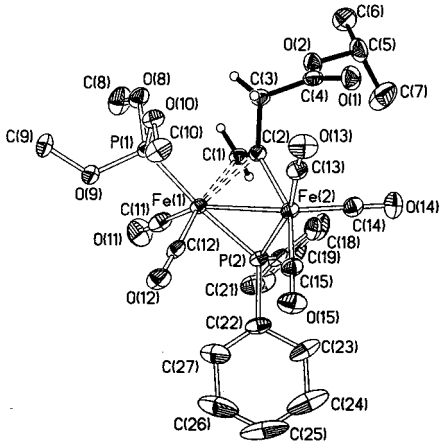

Figure 4. Molecular structure of $[Fe_2(CO)_5\{P(OMe)_3\}(\mu\text{-}PPh_2)(\mu\text{-}\eta^1\text{:}\eta^2\text{-}\{^iPrO(O)CCH_2\}C{=}CH_2)]$ (**3c**) with atom labels and 50% probability ellipsoid. Phenyl, methyl, and isopropyl H atoms are omitted for clarity.

(17) (a) Hogarth, G. *J. Organomet. Chem.* **1991**, *407*, 91. (b) Hogarth, G.; Lavender, M. H.; Shukri, K. *Organometallics* **1995**, *14*, 2325.

(18) Seyferth, D.; Hoke, J. B.; Womack, G. B. *Organometallics* **1990**, *9*, 2662.

Table 5. Selected Bond Distances (Å) and Angles (deg) for Compound 3c

Fe(1)−Fe(2)	2.6101(6)	Fe(1)−C(1)	2.152(3)
Fe(1)−C(2)	2.122(3)	Fe(1)−P(1)	2.1736(9)
Fe(1)−P(2)	2.2357(9)	Fe(1)−C(11)	1.791(4)
Fe(1)−C(12)	1.762(4)	Fe(2)−C(2)	1.987(3)
Fe(2)−P(2)	2.2151(10)	Fe(2)−C(13)	1.806(4)
Fe(2)−C(14)	1.768(4)	Fe(2)−C(15)	1.803(4)
C(1)−C(2)	1.395(5)	C(2)−C(3)	1.541(5)
C(3)−C(4)	1.514(5)	C(4)−O(1)	1.200(4)
C(4)−O(2)	1.342(4)		
P(1)−Fe(1)−P(2)	170.76(4)	C(1)−C(2)−C(3)	113.6(3)
C(2)−C(3)−C(4)	105.7(3)	O(1)−C(4)−C(3)	125.8(3)
Fe(1)−P(2)−Fe(2)	71.81(3)		

the trimethyl phosphite adopts a *trans* disposition with respect to the phosphido bridge (P(1)−Fe(1)−P(2) = 170.76(4)°). On the basis of direct substitution of the ester carbonyl oxygen−iron interaction, and retention of configuration, we would expect the phosphine to be coordinated to Fe(2). However, in the solid state the trimethyl phosphite is located on Fe(1), to which the alkenyl ligand is π-bonded. Preferential formation of this substitutional isomer is likely to be electronic in origin, presumably a reflection of the σ-donor−π-acceptor ability of the alkenyl ligand. As with **2c** the alkenyl group adopts an *endo* conformation with respect to the phosphido bridge, presumably minimizing unfavorable steric interactions between the ester substituent on C_β and the phenyl rings of the phosphido bridge.

Conclusion

Nucleophilic addition of alcohols to **1a,b** affords a convenient route to the binuclear σ-η^2-coordinated β,γ-unsaturated esters $[Fe_2(CO)_5(\mu\text{-}PPh_2)(\mu\text{-}\eta^1(O):\eta^1(C):\eta^2\text{-}(C)\text{-}\{R^1O(O)CCHR\}C{=}CH_2)]$ (**2a**, R^1 = Me; **2b**, R^1 = Et; **2c**, R^1 = ^{i}Pr**)**. Their synthesis *via* alcohol−allenyl−carbonyl coupling provides an alternative to that recently developed by Thomas and co-workers which involves nucleophilic attack at C1 of a (vinylketene)-tricarbonyliron(0) complex.[5a] Deuterium and substitutional labeling studies suggest a mechanism involving carbon−carbon bond formation between an OR-functionalized carbonyl and C_α of the allenyl ligand; the final product resulting from stereoselective hydrogen transfer to C_α. The selectivity of alcohols for this reaction pathway is quite remarkable and contrasts sharply with previous reports in which the reactivity of μ-η^1:η^2-binuclear allenyl complexes is dominated by nucleophilic attack at C_β.[19] Trimethyl phosphite readily displaces the metal-coordinated ester carbonyl in **2a**−**c** to afford the ester-functionalized μ-η^1:η^2-alkenyl complexes $[Fe_2(CO)_5\{P(OMe)_3\}(\mu\text{-}PPh_2)(\mu\text{-}\eta^1:\eta^2\text{-}\{R^1O(O)CCH_2\}C{=}CH_2)]$ (**3a**, R^1 = Me; **3b**, R^1 = Et; **3c**, R^1 = ^{i}Pr). These studies suggest strategies that could, if successful, create new opportunities for binuclear μ-η^1:η^2-allenyl complexes in organic synthesis. We are currently investigating other carbon−carbon and carbon−heteroatom coupling reactions of **1a** and its derivatives to fulfill this goal.

Experimental Section

General Procedures. Unless otherwise stated all manipulations were carried out in an inert atmosphere glove box or by using standard Schlenk line techniques. Diethyl ether and hexane were distilled from Na/K alloy, tetrahydrofuran from potassium, and dichloromethane from CaH_2. $CDCl_3$ was predried with CaH_2 and vacuum transferred and stored over 4 Å molecular sieves. Infrared spectra were recorded on a Mattson Genesis FTIR spectrometer operating WINFIRST software. Prop-2-yne bromide was purchased from Aldrich Chemical Co. and used without further purification. 3-Phenyl-2-propyn-1-yl bromide was prepared from 3-Phenyl-2-propyn-1-ol according to a literature procedure.[21] Reagent grade methanol and 2-propanol was used without further purification. Column chromatography was carried out with alumina purchased from Aldrich Chemical Co. and deactivated with 6% w/w water. The allenyl complex $[Fe_2(CO)_6(\mu\text{-}PPh_2)\{\mu\text{-}\eta^1:\eta^2_{\alpha\beta}\text{-}(H)C_\alpha{=}C_\beta{=}C_\gamma H_2\}]$ was prepared as previously described.[9]

Preparation of $[Fe_2(CO)_5(\mu\text{-}PPh_2)(\mu\text{-}\eta^1(O):\eta^1(C):\eta^2(C)\text{-}\{MeO(O)CCH_2\}C{=}CH_2)]$ (2a). An excess of methanol (3.0 mL) was added to a solution of $[Fe_2(CO)_6(\mu\text{-}PPh_2)\{\mu\text{-}\eta^1:\eta^2_{\alpha\beta}\text{-}(H)C_\alpha{=}C_\beta{=}C_\gamma H_2\}]$ (0.150 g, 0.30 mmol) in diethyl ether (20 mL), and the reaction mixture was stirred overnight during which time the color changed from pale yellow to deep red. The progress of the reaction was monitored by IR spectroscopy and thin layer chromatography which indicated a smooth conversion to **2a**. The solvent was removed, and the oily residue was dissolved in the minimum amount of dichloromethane, absorbed onto silica gel, placed on a 300 × 20 mm silica gel column, and eluted with hexane/dichloromethane (70:30, v/v) to afford a single red band corresponding to **2a**. The collected fraction was concentrated and cooled overnight at −20 °C to afford deep red crystals of **2a** in 70% yield (0.110 g). IR(ν(CO), cm^{-1}, C_6H_{14}): 2034 m, 1999 s, 1967 m, 1953 w, 1934 m, 1656 w. $^{31}P\{^1H\}$ NMR (202.5 MHz, $CDCl_3$, δ): 177.5 (s, μ-PPh_2). ^1H NMR (500.1 MHz, $CDCl_3$, δ): 7.4−7.1 (m, 10H, C_6H_5), 4.12 (dd, $^2J_{HH}$ = 21.7 Hz, $^4J_{PH}$ = 2.7 Hz, 1H, CH_cH_d), 3.75 (s, 3H, OCH_3), 3.21 (dd, $^3J_{PH}$ = 11.5 Hz, $^2J_{HH}$ = 2.9 Hz, 1H, CH_aH_b), 3.06 (dd, $^2J_{HH}$ = 21.7 Hz, $^4J_{PH}$ = 2.7 Hz, 1H, CH_cH_d), 2.20 (dd, $^3J_{PH}$ = 7.0 Hz, $^2J_{HH}$ = 2.9 Hz, 1H, CH_aH_b). $^{13}C\{^1H\}$ NMR (125.7 MHz, $CDCl_3$, δ): 217.2 (d, $^2J_{PC}$ = 12.6 Hz, CO), 214.9 (d, $^2J_{PC}$ = 2.5 Hz, CO), 213.2 (d, $^2J_{PC}$ = 15.1 Hz), 186.6 (s, $C(O)OCH_3$), 166.8 (d, $^2J_{PC}$ = 27.6 Hz, $CH_2{=}CCH_2$), 140−127 (m, C_6H_5), 63.1 (d, $^2J_{PC}$ = 8.8 Hz, $CH_2{=}CCH_2$), 54.7 (s, $C(O)OCH_3$), 53.4 (d, $^3J_{PC}$ = 3.7 Hz, $CH_2C(O)OCH_3$). MS (*m*/*z*, 70 EV): 536 (M^+), 508 (M^+ − CO), 480 (M^+ − 2CO), 452 (M^+ − 3CO), 424 (M^+ − 4CO), 396 (M^+ − 5CO). Anal. Calcd for $C_{22}H_{17}O_7PFe_2$: C; 49.30; H, 3.19. Found: C, 49.05; H, 3.01.

Compounds **2b** and **2c** were prepared using a procedure similar to that described above for **2a**. Selected spectroscopic and analytical data are listed for both compounds.

Preparation of $[Fe_2(CO)_5(\mu\text{-}PPh_2)(\mu\text{-}\eta^1(O):\eta^1(C):\eta^2(C)\text{-}\{EtO(O)CCH_2\}C{=}CH_2)]$ (2b). Obtained as deep red crystals in 77% yield from dichloromethane/*n*-hexane at room temperature. IR(ν(CO), cm^{-1}, C_6H_{14}): 2033 m, 1998 s, 1967 m, 1952 w, 1935 m, 1650 w. $^{31}P\{^1H\}$ NMR (202.5 MHz, $CDCl_3$, δ): 176.6 (s, μ-PPh_2). ^1H NMR (500.1 MHz, $CDCl_3$, δ): 7.4−7.1 (m, C_6H_5, 10H), 4.22 (ABq, $^2J_{HH}$ = 9.0 Hz, $^3J_{HH}$ = 7.1 Hz, 1H, CH_2CH_3), 5.15 (ABq, $^2J_{HH}$ = 9.0 Hz, $^3J_{HH}$ = 7.1 Hz, 1H, CH_2CH_3), 4.11 (br d, $^2J_{HH}$ = 21.2 Hz, 1H, CH_cH_d,), 3.21 (dd, $^3J_{PH}$ = 11.4 Hz, $^3J_{HH}$ = 2.9 Hz, 1H, CH_aH_b), 3.03 (dd, $^2J_{HH}$ = 21.2 Hz, $^4J_{PH}$ = 2.8 Hz, 1H, CH_cH_d), 2.21 (dd, $^3J_{PH}$ = 7.4 Hz, $^2J_{HH}$ = 2.9 Hz, 1H, CH_aH_b), 1.18 (t, $^3J_{HH}$ = 7.1 Hz, 3H, CH_2CH_3).

(19) For a selection of recent examples: (a) Baize, M. W.; Blosser, P. W.; Plantevin, V.; Schimpff, D. G.; Gallucci, J. C.; Wojcicki, A. *Organometallics* **1996**, *15*, 164. (b) Baize, M. W.; Plantevin, V.; Gallucci, J. C.; Wojcicki, A. *Inorg. Chim. Acta*. **1995**, *235*, 1. (c) Ogoshi, S.; Tsutsumi, K.; Kurosawa, H. *J. Organomet. Chem*. **1995**, *493*, C19. (d) Breckenridge, S. M.; Taylor, N. J., Carty, A. J. *Organometallics* **1991**, *10*, 837. (e) Huang, T.-M.; Chen. J.-T.; Lee, G.-H.; Wang, Y. *J. Am. Chem. Soc*. **1993**, *115*, 1170. (f) Blosser, P. W.; Schimpff, D. G.; Gallucci, J. C.; Wojcicki, A. *Organometallics* **1993**, *12*, 1993.

(20) Brandsma, L.; Verkruijsse, H. D. *Syntheses of Acetylenes, Allenes and Cumulenes*; Elsevier: Amsterdam, 1981; p 219.

(21) SMART and SAINT software for CCD diffractometer systems Siemens Analytical X-ray Instruments Inc., Madison, WI, 1994.

Table 6. Summary of Crystal and Intensity Data for Compounds 2c, 2d, and 3

compound	**2c**	**2d**	**3c**·$^7/_6$hexane
molecular formula	$C_{24}H_{21}Fe_2O_7P$	$C_{28}H_{21}Fe_2O_7P$	$C_{27}H_{30}Fe_2O_{10}P_2 \cdot {}^7/_6C_6H_{14}$
fw	564.1	612.1	788.7
temp (K)	160	160	160
cryst syst	triclinic	triclinic	rhombohedral
space group	$P\bar{1}$	$P\bar{1}$	$R\bar{3}$
a, Å	8.6234(13)	10.5803(14)	47.491(2)
b, Å	9.2037(15)	11.9135(16)	
c, Å	16.156(3)	12.5937(17)	9.1697(4)
α, deg	79.280(4)	62.558(3)	
β, deg	81.844(4)	71.580(3)	
γ, deg	78.504(3)	85.515(3)	
V, Å^3	1227.2(3)	1332.3(3)	17910.3(13)
Z	2	2	18
D_{calc}, g cm^{-3}	1.526	1.526	1.316
μ(Mo Kα), cm^{-1}	12.89	11.94	8.59
cryst size, mm	0.32 × 0.11 × 0.04	0.73 × 0.16 × 0.07	0.40 × 0.25 × 0.19
transm coeff range	0.764−0.954	0.823−0.927	0.786−0.942
scan range (2*θ*), deg	4.6−57.1	3.8−56.9	1.7−52.0
no. of rflns measured	7595	8172	33413
no. of unique rflns	5324	5730	7828
R_{int}	0.0345	0.0260	0.0502
weighting parameters[a] *a*, *b*	0.0396, 0.7302	0.0250, 1.4291	0.0573, 78.4655
extinction coeff *x*[b]	0.0035(8)	0.0010(5)	0.00055(4)
no. of variables	316	351	406
R_w (all data)[c]	0.0956	0.0811	0.1423
R ("observed" data)[d]	0.0399 (3987)	0.0347 (4721)	0.0529 (6833)
GOF[e]	1.047	1.081	1.257
Max. min el density, e Å^{-3}	0.400. −0.457	0.404, −0.303	1.129, −0.432

[a] $\omega^{-1} = \sigma^2(F_o^2) + (aP)^2 + bP$, where $P = (F_o^2 + 2F_c^2)/3$. [b] $F_c' = F_c(1 + 0.001xF_c^2\lambda^3/\sin 2\theta)^{-1/4}$. [c] $R_w = \{\sum[\omega(F_o^2 - F_c^2)^2]/\sum[\omega(F_o^2)^2]\}^{1/2}$ for all data. [d] $R = \sum||F_o| - |F_c||/\sum|F_o|$ for reflections having $F_o^2 > 2\sigma(F_o^2)$. [e] GOF = $[\sum\omega(F_o^2 - F_c^2)^2/(\text{no. of unique rflns} - \text{no. of variables})]^{1/2}$.

$^{13}C\{^1H\}$ NMR (125.7 MHz, $CDCl_3$, *δ*): 217.3 (d, $^2J_{PC}$ = 12.6 Hz, CO), 215.0 (d, $^2J_{PC}$ = 2.5 Hz, CO), 213.1 (d, $^2J_{PC}$ = 15.2 Hz, CO), 186.3 (s, *C*(O)OEt), 166.8 (d, $^2J_{PC}$ = 28.9 Hz, $CH_2{=}CCH_2$), 140−127 (m, C_6H_5), 64.5 (s, CH_2CH_3), 63.1 (d, $^2J_{PC}$ = 8.8 Hz, $CH_2{=}CCH_2$), 53.8 (d, $^3J_{PC}$ = 3.8 Hz, $CH_2C(O)$-OEt), 13.9 (br, s, CH_2CH_3). Anal. Calcd for $C_{23}H_{19}O_7PFe_2$: C, 50.19; H, 3.48. Found: C, 50.24; H, 3.25.

Preparation of [Fe$_2$(CO)$_5$(μ-PPh$_2$)(μ-η^1(O):η^1(C):η^2(C)-{^{i}PrO(O)CCH$_2$}C=CH$_2$)] (2c). Crystals suitable for X-ray analysis were obtained from dichloromethane/*n*-hexane at room temperature in 67% overall yield. IR(*ν*(CO), cm^{-1}, C_6H_{14}): 2032 m, 1998 s, 1967 m, 1951 w, 1934 m, 1641 w. $^{31}P\{^1H\}$ NMR (202.5 MHz, $CDCl_3$, *δ*): 176.9 (s, *μ*-PPh_2). ^1H NMR (500.1 MHz, $CDCl_3$, *δ*): 7.5−7.1 (m, C_6H_5, 10H), 5.03 (sept, $^3J_{HH}$ = 6.3 Hz, 1H, $CH(CH_3)_2$), 4.12 (dd, $^2J_{HH}$ = 21.3 Hz, $^4J_{PH}$ = 2.7 Hz, 1H, CH_cH_d), 3.31 (dd, $^3J_{PH}$ = 11.4 Hz, $^2J_{HH}$ = 2.9 Hz, 1H, CH_aH_b), 2.97 (dd, $^2J_{HH}$ = 21.3 Hz, $^4J_{PH}$ = 2.7 Hz, 1H, CH_cH_d), 2.21 (dd, $^3J_{PH}$ = 6.6 Hz, $^2J_{HH}$ = 2.9 Hz, 1H, CH_aH_b), 1.22 (d, $^3J_{HH}$ = 6.3 Hz, 3H, $CH(CH_3)_2$), 1.14 (d, $^3J_{HH}$ = 6.3 Hz, 3H, $CH(CH_3)_2$). $^{13}C\{^1H\}$ NMR (125.7 MHz, $CDCl_3$, *δ*): 217.4 (d, $^2J_{PC}$ = 11.3 Hz, CO), 215.0 (d, $^2J_{PC}$ = 2.5 Hz, CO), 213.2 (d, $^2J_{PC}$ = 15.1 Hz), 186.0 (s, *C*(O)OCH(CH$_3$)$_2$), 166.8 (d, $^2J_{PC}$ = 27.7 Hz, $CH_2{=}CCH_2$), 140−127 (m, C_6H_5), 73.0 (s, $CH(CH_3)_2$), 63.3 (d, $^2J_{PC}$ = 8.8 Hz, $CH_2{=}CCH_2$), 54.2 (d, $^3J_{PC}$ = 3.5 Hz, $CH_2C(O)O^iPr$), 21.5 (s, $CH(CH_3)_2$). MS (*m*/*z*, 70 eV): 564 (M$^+$), 536 (M$^+$ − CO), 508 (M$^+$ − 2CO), 480 (M$^+$ − 3CO), 452 (M$^+$ − 4CO), 424 (M$^+$ − 5CO). Anal. Calcd for $C_{24}H_{21}O_7PFe_2$: C, 51.11; H, 3.70. Found: C, 50.89; H, 3.20.

Preparation of [Fe$_2$(CO)$_5$(μ-PPh$_2$)(μ-η^1(O):η^1(C):η^2(C)-{MeO(O)CCHPh}C=CH$_2$)] (2d). The diiron allenyl complex [$Fe_2(CO)_6$(*μ*-PPh_2){*μ*-η^1:η$^2_{\alpha\beta}$-(Ph)C$_\alpha$=C$_\beta$=C$_\gamma$H$_2$}] (**1b**) was prepared *in situ* by stirring a diethyl ether solution of Na[Fe_2-(CO)$_7$(*μ*-PPh_2)] (0.200 g, 0.39 mmol) with 3-phenyl-2-propyn-1-yl bromide (0.151 mL, 0.78 mmol). After stirring overnight methanol was added and the reaction mixture stirred for a further 24 h during which time a deep red coloration appeared. The solvent was removed and the residue dissolved in the minimum amount of dichloromethane, absorbed onto neutral alumina, placed on a 300 × 20 mm alumina column, and eluted with hexane/dichloromethane (70:30, v/v) to afford a prominent red band corresponding to **2a**. The collected fraction was crystallized from dichloromethane/*n*-hexane at room temperature to afford deep red X-ray quality crystals of **2a** (45%, 0.106 g). IR(*ν*(CO), cm^{-1}, C_6H_{14}): 2033 m, 1998 s, 1966 m, 1952 w, 1934 m, 1648 w. $^{31}P\{^1H\}$ NMR (202.5 MHz, $CDCl_3$, *δ*): 172.3 (s, *μ*-PPh_2). ^1H NMR (500.1 MHz, $CDCl_3$, *δ*): 7.4−7.1 (m, 15H C_6H_5), 5.12 (br, s, 1H, C*H*Ph), 3.26 (s, 3H, OCH_3), 2.60 (dd, $^2J_{PH}$ = 11.4 Hz, $^2J_{HH}$ = 3.7 Hz, 1H, CH_aH_b), 2.23 (ddd, $^3J_{PH}$ = 7.6 Hz, $^2J_{HH}$ = 3.7 Hz, $^3J_{HH}$ = 1.5 Hz, 1H, CH_aH_b). $^{13}C\{^1H\}$ NMR (125.7 MHz, $CDCl_3$, *δ*): 217.1 (d, $^2J_{PC}$ = 12.6 Hz, CO), 215.6 (d, $^2J_{PC}$ = 3.8 Hz, CO), 214.7 (d, $^2J_{PC}$ = 3.8 Hz, CO), 211.9 (d, $^2J_{PC}$ = 13.8 Hz, CO), 185.2 (s, *C*(O)OCH_3), 171.0 (d, $^2J_{PC}$ = 21.3 Hz, $CH_2{=}CCHPh$), 140−127 (m, C_6H_5), 68.9 (d, $^2J_{PC}$ = 7.6 Hz, $CH_2{=}CCH_2$), 53.5 (s, C(O)OCH_3), 52.3 (d, $^3J_{PC}$ = 3.8 Hz, $CH_2C(O)CH_3$).

Preparation of [Fe$_2$(CO)$_5${P(OMe)$_3$}(μ-PPh$_2$)(μ-η^1:η^2-{MeO(O)CCH$_2$}C=CH$_2$)] (3a). Addition of trimethyl phosphite (0.09 mL, 7.7 mmol) to a solution of **2a** (0.125 g, 0.25 mmol) in diethyl ether (20 mL) led to a gradual color change from the characteristic intense cherry red to golden yellow. The reaction mixture was stirred under dinitrogen for 6 h after which time the solvent was removed to leave an oily residue. This residue was taken up in the minimum volume of dichloromethane, absorbed onto alumina, placed on a 300 × 20 mm alumina column, and eluted with *n*-hexane/dichloromethane (30:70, v/v) to afford a single major band corresponding to **3a** (120 mg, 72%). IR(*ν*(CO), cm^{-1}, C_6H_{14}): 2044 s, 1981 s, 1975 s, 1965 s, 1928 w, 1735 w. $^{31}P\{^1H\}$ NMR (202.5 MHz, $CDCl_3$, *δ*): 177.4 (d, $^2J_{PP}$ = 90.9 Hz, P(OMe)$_3$), 169.8 (d, $^2J_{PP}$ = 90.9 Hz, *μ*-PPh_2). ^1H NMR (500.1 MHz, $CDCl_3$, *δ*): 7.6−7.1 (m, 10H, C_6H_5), 4.22 (d, $^2J_{HH}$ = 12.2 Hz, 1H, CH_cH_d), 3.73 (s, 3H, C(O)OCH_3), 3.59 (d, $^3J_{PH}$ = 11.1 Hz, 9H, P(OCH_3)$_3$), 3.05 (d, $^2J_{HH}$ = 12.2 Hz, 1H, CH_cH_d), 2.72 (d, br, $^3J_{PH}$ = 15.5 Hz, $^2J_{HH}$ = 4.0 Hz, 1H, CH_aH_b), 2.17 (ddd, br, $^3J_{PH}$ = 8.9 Hz, 1H, CH_aH_b). $^{13}C\{^1H\}$ NMR (125.7 MHz, $CDCl_3$, *δ*): 216.9 (dd, $^2J_{PC}$ = 20.5 Hz, CO), 215.2 (dd, $^2J_{PC}$ = 37.0 Hz, $^2J_{PC}$ = 5.6 Hz CO), 212.0 (s, br, CO), 178.5 (d, $^2J_{PC}$ = 21.9 Hz, $CH_2{=}CCH_2$), 172.8 (s, CH_2(O)OCH_3), 140−127 (m, C_6H_5), 71.2 (dd, $^2J_{PC}$ = 14.9 Hz, $^2J_{PC}$ = 5.6 Hz, $CH_2{=}CCH_2$), 61.6 (d, $^3J_{PC}$ = 6.6 Hz, $CH_2C(O)$-OCH_3), 52.6 (d, $^3J_{PC}$ = 5.1 Hz, P(OCH_3)$_3$), 52.4 (s, C(O)OCH_3).

Compounds **3b** and **3c** were prepared using a procedure similar to that described for **3a**.

Preparation of $[Fe_2(CO)_5\{P(OMe)_3\}(\mu\text{-}PPh_2)(\mu\text{-}\eta^1{:}\eta^2\text{-}\{EtO(O)CCH_2\}C{=}CH_2)]$ (3b). Obtained as deep orange crystals from a concentrated hexane solution at room temperature; overall yield 54%. IR(ν(CO), cm^{-1}, C_6H_{14}): 2044 s, 1981 s, 1975 s, 1965 s, 1927 w, 1741 w. $^{31}P\{^1H\}$ NMR (202.5 MHz, $CDCl_3$, δ): 176.2 (d, $^2J_{PP}$ = 88.0 Hz, $P(OMe)_3$), 166.8 (d, $^2J_{PP}$ = 88.0 Hz, μ-PPh_2). ^1H NMR (500.1 MHz, $CDCl_3$, δ): 7.6−7.1 (m, 10H, C_6H_5), 4.22 (d, $^2J_{HH}$ = 12.3 Hz, 1H, CH_cH_d), 4.18 (q, $^3J_{HH}$ = 7.1 Hz, 2H, CH_2CH_3), 3.59 (d, $^3J_{PH}$ = 11.1 Hz, 9H, $P(OCH_3)_3$), 3.05 (d, $^2J_{HH}$ = 12.3 Hz, 1H, CH_cH_d), 2.71 (ddd, $^3J_{PH}$ = 15.7 Hz, $^3J_{PH}$ = 7.2 Hz, $^2J_{HH}$ = 3.1 Hz, 1H, CH_aH_b), 2.15 (ddd, $^3J_{PH}$ = 11.8 Hz, $^3J_{PH}$ = 9.1 Hz, $^2J_{HH}$ = 3.1 Hz, 1H, CH_aH_b), 1.27 (t, $^3J_{HH}$ = 7.1 Hz, 3H, CH_2CH_3). $^{13}C\{^1H\}$ NMR (125.7 MHz, $CDCl_3$, δ): 216.6 (dd, $^2J_{PC}$ = 20.5 Hz, CO), 215.2 (dd, $^2J_{PC}$ = 35.6 Hz, $^2J_{PC}$ = 6.1 Hz CO), 212.0 (s, br, CO), 178.9 (d, $^2J_{PC}$ = 21.9 Hz, $CH_2{=}CCH_2$), 172.4 (s, $CH_2C(O)OEt$), 140−127 (m, C_6H_5), 71.3 (dd, $^2J_{PC}$ = 14.3 Hz, $^2J_{PC}$ = 5.6 Hz, $CH_2{=}CCH_2$), 62.2 (s, $CH_2C(O)OEt$), 60.8 (s, OCH_2CH_3), 52.6 (d, $^3J_{PC}$ = 5.1 Hz, $P(OCH_3)_3$), 14.2 (s, OCH_2CH_3).

Preparation of $[Fe_2(CO)_5\{P(OMe)_3\}(\mu\text{-}PPh_2)(\mu\text{-}\eta^1{:}\eta^2\text{-}\{^iPrO(O)CCH_2\}C{=}CH_2)]$ (3c). Crystals suitable for X-ray analysis were obtained from dichloromethane/*n*-hexane at room temperature in 92% overall yield. IR(ν(CO), cm^{-1}, C_6H_{14}): 2043 s, 1981 s, 1977 s, 1965 s, 1927 w, 1735 w. $^{31}P\{^1H\}$ NMR (202.5 MHz, $CDCl_3$, δ): 177.6 (d, $^2J_{PP}$ = 87.1 Hz, $P(OMe)_3$), 168.3 (d, $^2J_{PP}$ = 87.1 Hz, μ-PPh_2). ^1H NMR (500.1 MHz, $CDCl_3$, δ): 7.6−7.1 (m, 10H, C_6H_5), 5.02 (sept, $^2J_{HH}$ = 6.2 Hz, 1H, $CH(CH_3)_2$), 4.18 (d, $^2J_{HH}$ = 12.4 Hz, 1H, CH_cH_d), 3.60 (d, $^3J_{PH}$ = 11.1 Hz, 9H, $P(OCH_3)_3$), 3.02 (d, $^2J_{HH}$ = 12.4 Hz, 1H, CH_cH_d), 2.72 (ddd, $^3J_{PH}$ = 15.7 Hz, $^3J_{PH}$ = 7.0 Hz, $^2J_{HH}$ = 3.1 Hz, 1H, CH_aH_b), 2.18 (ddd, $^3J_{PH}$ = 11.7 Hz, $^3J_{PH}$ = 8.9 Hz, $^2J_{HH}$ = 3.2 Hz, 1H, CH_aH_b), 1.28 (d, $^3J_{HH}$ = 6.2 Hz, 3H, $CH(CH_3)_2$), 1.23 (d, $^3J_{HH}$ = 6.2 Hz, 3H, $CH(CH_3)_2$). $^{13}C\{^1H\}$ NMR (125.7 MHz, $CDCl_3$, δ): 217.0 (t, $^2J_{PC}$ = 21.3 Hz, CO), 215.3 (d, $^2J_{PC}$ = 35.2 Hz, CO), 179.1 (d, $^2J_{PC}$ = 21.4 Hz, $CH_2{=}CCH_2$), 171.9 (s, $C(O)O^iPr$), 140−127 (m, C_6H_5), 71.2 (dd, $^2J_{PC}$ = 14.2 Hz, $^2J_{PC}$ = 5.4 Hz, $CH_2{=}CCH_2$), 68.1 (s, $CH_2C(O)O^iPr$), 62.8 (s, $CH(CH_3)_2$), 52.5 (d, $^3J_{PC}$ = 6.2 Hz, $P(OCH_3)_3$), 21.8 (s, $CH(CH_3)_2$), 21.7 (s, $CH(CH_3)_2$). Anal. Calcd for $C_{27}H_{30}O_{10}P_2Fe_2$: C, 47.10; H, 4.39. Found: C, 47.16; H, 4.42.

Crystal Structure Determination of 2c, 2d, and 3c. Single crystals of each compound were obtained as described above. Crystals were examined on a Siemens SMART CCD area-detector diffractometer with graphite-monochromated Mo Kα radiation (λ = 0.71073 Å). Cell parameters were refined from the observed setting angles of all strong reflections in each complete data set. Intensities were integrated from series of ω-rotation exposures with different ϕ-angles chosen to generate more than a hemisphere of data, each exposure covering 0.3° in ω. Analysis of repeated and symmetry equivalent data indicated no significant intensity decay and formed the basis of empirical absorption corrections.

The structures were solved by direct methods and refined by full-matrix least-squares on F^2 values for all unique data (see Table 6 for details). All non-hydrogen atoms except for hexane solvent were assigned anisotropic displacement parameters. Hydrogen atoms were constrained to ideal positions with a riding model and with U_{iso}(H) set at 1.2 (1.5 for methyl groups) times U_{eq} for the parent atom, except for terminal alkene CH_2, for which positions were refined freely. For **3**, one hexane molecule of complex was located and refined with restraints on geometry and the U_{iso} values; hydrogen atoms were not included. There were indications of a further hexane molecule (approximately one per six molecules of complex) disordered on the crystallographic C_3 axis, but they could not be successfully modeled and were not included in the refinement. Programs used were Siemens SMART (control) and SAINT (integration) software,[21] SHELXTL,[22] and local programs, on Silicon Graphics Indy workstations and Personal Computer systems.

Acknowledgment. We thank the University of Newcastle upon Tyne for financial support for this work, the Nuffield foundation, and The Royal Society for grants (S.D.) and the EPSRC for funding for a diffractometer (W.C.).

Supporting Information Available: For **2c**, **2d**, and **3c** details of structure determination (Tables S1, S6, and S11), non-hydrogen atomic positional parameters (Tables S2, S7, and S12), full listings of bond distances and angles (Tables S3, S8, and S13), anisotropic displacement parameters (Tables S4, S9, and S14), and hydrogen atomic coordinates (Tables S5, S10, and S15) (18 pages). Ordering information is given on any current masthead page. Observed and calculated structure factor tables are available from the authors upon request.

OM960832Z

(22) Sheldrick, G. M. SHELXTL version 5, Siemens Analytical X-ray Instruments Inc., Madison, WI, 1995.